LAWRENCE
LIVERMORE
NATIONAL
LABORATORY

LLNL-CONF-850014

The WARP Reactor Concept

M. G. Anderson, J. K. Walters, E. M. Anaya, D. A. Max, W. A. Stygar, A. J. Link

June 7, 2023

2023 IEEE Pulsed Power Conference
San Antonio, TX, United States
June 25, 2023 through June 29, 2023

Disclaimer

The WARP Reactor Concept

Michael G. Anderson
National Security Engineering Division
Lawrence Livermore National Laboratory
Livermore, California, USA
anderson286@llnl.gov

James K. Walters
National Security Engineering Division
Lawrence Livermore National Laboratory
Livermore, California, USA
walters27@llnl.gov

Enrique M. Anaya
National Security Engineering Division
Lawrence Livermore National Laboratory
Livermore, California, USA
anaya1@llnl.gov

Don. A. Max
Mission Support and Test Services
Nevada National Security Site
Livermore Operations
Livermore, California, USA
max5@llnl.gov

William A. Stygar
National Security Engineering Division
Lawrence Livermore National Laboratory
Livermore, California, USA
stygar1@llnl.gov

Anthony J. Link
National Security Engineering Division
Lawrence Livermore National Laboratory
Livermore, California, USA
link6@llnl.gov

***Abstract*— The WARP Reactor Concept promises orders of magnitude increase of intense ion beam energies and respective radiation yields at a fraction of the size and cost over existing z-pinch class accelerators allowing the economically viable study of new Relativistic High Energy Density Physics regimes for probing the intersection between General Relativity and Quantum Field Theory along with game-changing direct applications from rep-rated Magnetized Liner Inertial Fusion devices for energy production and advanced propulsion to multi-pulse compact flash x-ray/neutron radiography sources for assessing our Nation's aging nuclear weapons stockpile. A brief overview of the WARP Reactor Concept is provided here with more in-depth treatment with additional figures and tables provided in the companion PPC2023 conference presentation.**

Keywords*— *warp reactor, particle accelerator, dense plasma focus, z-pinch, relativistic high energy density physics, quantum gravity, magnetized liner inertial fusion, advanced propulsion, compact flash x-ray and neutron source radiography

I. Introduction

The Wave Accelerated Ring Pinch or "WARP" Reactor [1,2] (patent pending), iso-view shown in Figure 1, is expected to solve key issues ranging from our present energy dependence on finite fossil fuels and its associated climate impact to our aging nuclear weapons stockpile. The WARP Reactor promises orders of magnitude increase of ultra-intense ion beam energies and respective high radiation yields at a fraction of the size and cost over other z-pinch class accelerators allowing the economically viable and environmental friendly study of new Relativistic High Energy Density (RHED) Physics regimes for probing the intersection between General Relativity and Quantum Field Theory (i.e. Warp/Unruh/Casimir effects) [3-6] along with game-changing direct applications from rep-rated Magnetized Liner Inertial Fusion (MagLIF) devices for energy production and advanced propulsion to multi-pulse compact flash x-ray/neutron radiography sources for assessing our Nation's aging nuclear weapons stockpile.

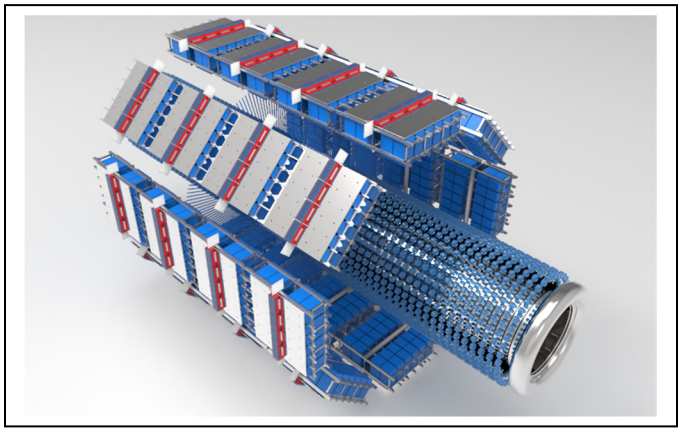

Fig. 1. Iso-view of The WARP Reactor

II. Novelty

The WARP Reactor utilizes state-of-the-art pulsed power modules to drive its "WARP Core" which consists primarily of two Dense Plasma Focuses (DPFs) and two Ion Ring Marx Generators (IRMGs) fired directly at one another. The WARP Reactor's dramatic performance boost is achieved with the use of a novel WARP Core which injects two tubular dense plasma and ion beams from opposite ends of a double-barreled DPF head with embedded IRMG-driven reflex triodes and through magnetic cusps into an axial seed B-field to form co-rotating ion rings which merge near the mid-plane of the device and are subsequently radially compressed and azimuthally accelerated up to 10^3 times the initial ion beam energies during the axial magnetic flux compression phase driven by the DPF plasma liner implosion. Two DPF and IRMG heads are implemented to

dramatically reduce the size and cost of the drivers and increase ion ring capture efficiency along with the added benefits of favorable magnetic field line curvature throughout implosion process due to higher velocity shear-stabilized DPF plasma pinch flows near each gun muzzle and greater tuning capability for properly timing the implosion and ion beam generation, injection and compression of the two colliding and subsequently merged ion rings onto a solid or high energy density plasma target.

III. Strategic Importance

WARP directly aligns with the DOE and NNSA missions and core competencies as an economically viable and climate-friendly rep-rated MagLIF device for nuclear fusion energy production as well as a multi-pulse compact flash x-ray/neutron source for assessing our aging nuclear weapons stockpile. In addition to developing the next-generation pulsed power architectures, this Strategic Initiative will help to benchmark present high-performance computing, simulation, and data science with respect to more disruptive and imaginative ultra-intense plasma/beam configurations. Finally, WARP success would fortify LLNL's place at the forefront of the subsequent RHED physics and technology revolution.

IV. WARP Reactor Physics

The WARP Reactor conceptual design, models, simulations, and targeted performance characteristics for the various applications pull directly from standard fusion plasma, beam, accelerator and relativistic physics along with a modified Einstein Field Equation (EFE) [5] and respective Figures Of Merit (FOM) for assessing the validity of a recently proposed Naïve Quantum Gravity (NQG) theory [6].

A. Ring Pinch and Acceleration Physics

The physics behind charged particle ring radial compression and azimuthal acceleration [7] in the WARP Core is as follows: Magnetic flux (Φ_z) compression (i.e. conservation of seed Φ_z during DPF z-pinch driven imploding liners: $\Phi_z = B_z\pi r^2$ = constant) creates a "Magnetic Wave" (i.e. seed B_z amplitude rapidly swells/increases since flux conservation dictates that $B_z \propto r^{-2}$) which forces (i.e. F = qV x B) charged particle rings to radially compress (i.e. decrease in Larmor radius: $r_L = \gamma m V_\theta/qB$) and due to the conservation of canonical angular momentum (i.e. $p_\theta = \gamma m r V_\theta + q\Phi_z/2\pi$ = constant) and adiabatic flux conservation condition (i.e. p_θ^2/B_z = constant or $p_\theta r$ = constant) the charged particle ring azimuthal velocities scale as: $V_\theta \propto (r_i/r_f)$ for $\gamma = 1$. Since Φ_z and p_θ are conserved in this device, final charged particle ring energy is: $E_f = \frac{1}{2}\gamma N m (V_{\theta f})^2 \sim E_i (r_i/r_f)^2$. Finally, for relativistic charged particle motion in pulsed B-fields, γ varies due to $\nabla \times \mathbf{E} = -(\delta \mathbf{B}/\delta t)$ and therefore $E_f \sim E_i (B_f/B_i)$.

B. Fusion Plasma Physics

The principal formulas used in the WARP Reactor conceptual models and simulations are the standard fusion plasma physics equations (1)-(11) in MKS units (unless specifically identified otherwise) for: N_n – the number of fusion-generated neutrons; β – plasma to magnetic pressure; E_f – total fusion energy; E_p – plasma energy; E_b – bremsstrahlung and E_s –synchrotron radiation energy; G_S – scientific and G_E – engineering gains; E_{sale} – fusion energy for sale; v_A – Alfvén velocity; τ_R – magnetic reconnection time scales along with plasma and particle beam propagation modes (i.e. $\beta > 1$ for diamagnetic drift mode; $\beta << 1$ for collective mode; $\beta << 1$ with polarization E-field shorted for single particle mode).

$$N_n \sim n^2 < \sigma v > V \tau \tag{1}$$

$$\beta = \frac{n k T}{B^2/2\mu_0} \tag{2}$$

$$E_f = N_n E_r \tag{3}$$

$$E_p = \frac{3}{2} n V k T \tag{4}$$

$$Eb \sim 10^{-38} Z^2 n^2 T[ev]^{0.5} V \tau \tag{5}$$

$$E_s \sim \frac{2Kq^2 \gamma^4 c}{3 r^2} N_e \tau \tag{6}$$

$$G_S = \frac{E_f}{E_p} \tag{7}$$

$$G_E = \frac{E_f}{E_T} \tag{8}$$

$$E_{sale} = f[E_f - E_p - E_b - E_s] \tag{9}$$

$$v_A = \frac{B}{\sqrt{\mu_0 \rho}} \tag{10}$$

$$\tau_R = \frac{L^2}{\delta v_A} \tag{11}$$

Where n is the plasma density; $< \sigma v >$ is the fusion reaction rate; V is the plasma/beam/ring volume; τ is the confinement time; k is the Boltzmann constant; T is plasma temperature; B is the magnetic field; μ_0 is the vacuum permeability; E_r is the fusion energy per reaction; Z is the atomic number; K is the Coulomb constant; q is the charge; γ is the Lorentz factor; c is the speed of light in vacuum; N_e is the number of electrons; E_T is the total stored energy of reactor; f is the conversion efficiency; ρ is the mass density; L is the half-length of current sheet; and δ is the current sheet half-thickness.

C. Relativistic Formulas, Modified EFE, NQG and FOM

In addition to the standard relativistic formulas for the Lorentz factor (12), momentum (13) and energy (14), we also introduce a modified EFE (15) with a NQG addition (16) that may be accessible by the WARP Reactor for verification or invalidation of the theory along with relevant FOM such as spacetime curvature (17), gravitational potential (18) and frame-dragging effects (19).

$$\gamma = \frac{1}{\sqrt{1 - \frac{v^2}{c^2}}} \tag{12}$$

$$\vec{p} = \gamma m \vec{v} \tag{13}$$

$$E = \gamma m c^2 \tag{14}$$

$$G_{\mu\nu} = \frac{8\pi G}{c^4}(S + A)\, T_{\mu\nu} \tag{15}$$

$$T_{\mu\nu} \rightarrow Re\left[\frac{\psi_f^{*}\, \hat{T}_{\mu\nu}\, \psi_i}{< f \mid i >}\right] \tag{16}$$

$$C_{\alpha\sigma} = (S + A)\frac{G\,M}{c^2\,V} \tag{17}$$

$$\Phi_{\alpha\sigma} = (S + A)\frac{G\,M}{c^2\,R} \tag{18}$$

$$\Omega_{\alpha\sigma} = (S + A)\frac{G\,I\,\omega}{c^2\,R^3} \tag{19}$$

$G_{\mu\nu}$ - Einstein curvature tensor; $T_{\mu\nu}$ - energy-momentum tensor; $8\pi G/c^4$ - energy-momentum to curvature coupling constant in vacuum; G - Newton's gravitational constant; "S" - Sarfatti plasma metamaterial effects; "A" - Anderson Unruh/Casimir threshold effects; $T_{\mu\nu}$ - Sutherland NQG addition; $\hat{T}_{\mu\nu}$ - energy-momentum operator; ψ_i and ψ_f^{*} - initial and final conjugate wavefunctions, respectively; $< f \mid i >$ - final and initial boundary conditions; FOM: $C_{\alpha\sigma}$ - spacetime curvature; $\Phi_{\alpha\sigma}$ - gravitational potential and $\Omega_{\alpha\sigma}$ - frame-dragging effect; M - ring mass; R - ring radius; I – ring moment of inertia; ω – ring angular velocity.

V. WARP Reactor Technology

The WARP Reactor utilizes tried-and-true Shiva Star-like "TEMPEST" Marx Modules to drive its dual Dense Plasma Focus head and state-of-the-art Impedance-matched Marx Generators [8] (or Linear Transformer Drivers for rapid rep-rate operation [9]) to drive the dual charged particle beam-ring reflex triodes. Figures 2 shows a cross-sectional view of the full-scale WARP Reactor. The WARP Reactor consists primarily of 40 TEMPEST modules, 2 Ion Ring Marx Generators and the central WARP Core.

A. TEMPEST Marx Modules

Forty TEMPEST Marx modules drive the dual DPF heads. A cross-sectional view of a single TEMPEST Marx module is provided in Figure 3 which consists of a more robust version of the Shiva Star design with upgraded 1.2MA railgap switches, a seismically-rated welded frame capacitor assembly along with a modified HV output header for the flexible high current coaxial cable connections. Each TEMPEST Module is primarily comprised of four super-duty railgap switches, aluminum parallel plate transmission lines and twenty-four +/-60kV, 250kA high energy density capacitors with a total energy stored per module of ~260kJ and a total 40 module TEMPEST system storage of >10MJ and capable of delivering ~60MA to the DPF loads.

B. Ion Ring Marx Generators

Two IRMGs drive the dual Reflex Triode heads. For single pulse operation, each IRMG is a 30-stage Impedance-matched Marx Generator (IMG) on steroids or a Linear Transformer Driver (LTD) for rapid rate-rate operation. The IMG-version,

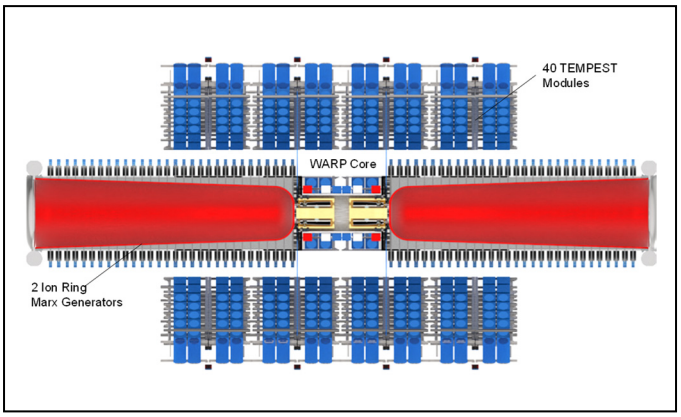

Fig. 2. Cross-sectional view of The WARP Reactor showing TEMPEST Modules, IRMGs and WARP Core (total machine size: ~18m x ~9m)

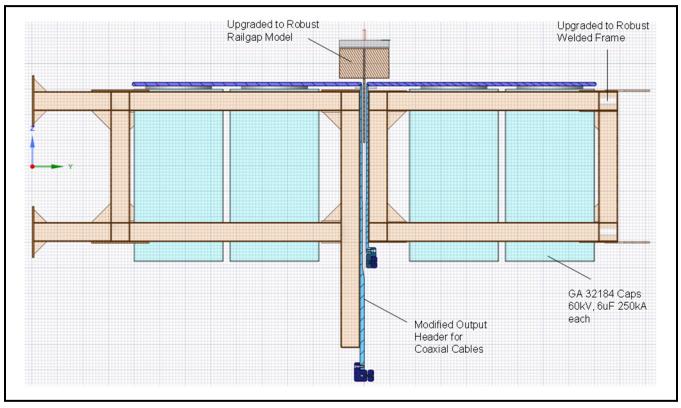

Fig. 3. Cross-sectional view of TEMPEST Marx module

cross-sectional view shown in Figure 4, consists primarily of 30 segmented coaxial return spools, a continuous tapered inner HV stalk, corona toroid, and 40 bricks per stage with each brick being comprised of two capacitors and a high-performance spark-gap switch. Each IRMG can produce a ~1MV, ~1MA, ~100ns pulse to the Reflex Triode with a total energy storage for a two-IRMG system of ~2MJ.

C. WARP Core

Depicted in Figure 5 is a cross-sectional view of the novel WARP Core (~1m L end-to-end x ~0.5m diameter at B-magnets). The relatively large Red, White and Blue squares situated around the grounded vacuum chamber represent the B-insulation, B-Seed and B-cusp pulsed magnets. Whereas the small blue squares (next to the magnets) and internal light blue rectangles are the annular DPF and IRMG puff valves, respectively. The TEMPEST Modules attach to the WARP Core at the DPF Collection Plates on the Left and Right End of the Device. Whereas the Ion Ring Marx Generators connect to the two back-ends of the dual Reflex Triodes through the IRMG Post-hole convolutes. Finally, the primary WARP Core and most novel central components consist of coaxial dual DPF (~13cm diameter) and IRMG heads with embedded Reflex Triodes (~10cm diameter).

VI. WARP Reactor Machine Metrics

WARP Reactor major pulsed power parameters, DPF plasma liner and Ion Beam/Ring metrics are provided in the conference

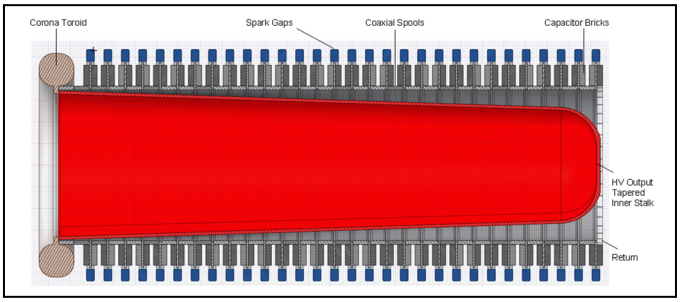

Fig. 4. Cross-sectional view of Ion Ring Marx Generator (IMG-version)

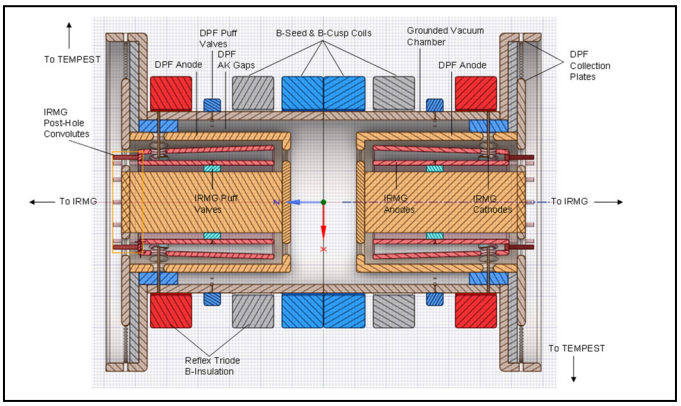

Fig. 5. Cross-sectional view of the WARP Core

presentation along with a table comparing several WARP devices to one of the largest particle beam accelerators in recent times, PBFA II [10]. With respect to PBFA II (predecessor to the Z-Machine), the 60MA WARP Reactor shows an order of magnitude increases in ion beam energy (GeV-level) and beam/ring current (20MA at implosion stagnation) with 25% acceleration efficiencies.

VII. WARP Reactor Operations

WARP Reactor operations can be separated into five major phases. PHASE 1 begins with the creation of the B-insulation, B-seed and B-cusp magnetic fields to ensure full B-field diffusion through the metal structures along with gas injection via the DPF and IRMG annular puff valves and subsequent firing of the TEMPEST modules to initiate dual DPF plasmoid generation, lift-off and run-down. PHASE 2 occurs as the two DPFs begin their run-in sequence and the IRMGs are fired to produce the dual tubular ion beams. PHASE 3 is when the DPFs return currents have merged and the dual axially directed ion beams have passed through their respective B-cusp fields to become co-rotating and merged ion rings in the embedded B-seed field. PHASE 4 is the DPF plasma liner implosion sequence which provide the necessary flux compression and subsequent ion ring pinch and azimuthal acceleration. PHASE 5 is the implosion stagnation phase and relativistic high energy density ion ring and target interaction sequence for fusion energy production, advanced propulsion, super-flash x-ray and neutron generation for radiographic and/or dynamic interrogation applications and/or accessing new RHED physics regimes. To further aid in visualizing the WARP Core Operations we have provided a movie embedded within the conference presentation which also identifies the respective phases.

VIII. WARP Reactor Models and Simulations

To help benchmark our WARP Reactor's plasma liner implosion simulations we compare them to a Semi-Analytical Model for Magnetized Liner Inertial Fusion [11], which can be used to reproduce the general 1D behavior of MagLIF machines. This model provides many key aspects of MagLIF, including: (1) fuel preheat; (2) liner implosion; (3) liner compressibility, internal magnetic pressure, and ohmic heating; (4) adiabatic heating by compression; (5) fuel opacity and radiative loss; (6) B-flux compression with; (7) magnetized electron and ion thermal conduction losses; (8) end losses; (9) enhanced losses due to mixing; (10) D-D and D-T primary fusion reactions for fuel ratios; and (11) α-particle fuel heating. However, to expedite comparisons between our multi-physics models/simulations and semi-analytical models, we have created a simplified version of the MagLIF model in Mathematica which also allows rapid exploration of WARP Reactor parameter space for performance optimization.

In addition to the multi-physics models and simulations we have created 3D Computer Aided Design (CAD) engineering models with associated Finite Element Analysis (FEA) for electrical and mechanical stresses along with circuit models and simulations for the TEMPEST system, IRMGs (both for single-pulse IMG and rep-rated LTD varieties) and WARP Core dynamic loads.

A simulation effort was performed for a mini-WARP Core in the Chicago particle-in-cell code in hybrid-kinetic mode where the electrons are treated as an inertia-less fluid using MHD equations for the electron response while the ions are treated as kinetic particles. Simulation results are again provided in the conference presentation.

A. DPF & Ion Beam Propagation Mechanisms

References [12,13] provide detailed propagation criteria for plasma/beam transport across magnetic field lines in vacuum or background magnetized plasma. Provided in the conference presentation are tables showing the DPF plasmoid initial characteristics and propagation via the diamagnetic drift mode while the ion beam propagates in the collective mode until the polarization E-field is shorted by background electrons. The reflex triode and initial ion beam parameters are also provided along with final compression and accelerations. Of particular interest to Warp, Unruh, dynamic Casimir and QG effects, the electron ring mode of operation indicates submicron implosion radii and $>10^{23}$ m/s^2 azimuthal accelerations depending on initial e-beam and magnetic flux parameters.

B. DPF Plasmoids Magnetic Reconnection

The DPF plasmoids diamagnetic drift or "plow-through" the B-Cusp field region (i.e. as hot-knives through butter) with magnetic reconnection and subsequent plasmoids collision at the midplane of the WARP Core on microsecond time scales.

C. Compression, Acceleration, Fusion & Radiation Metrics

Ring compression and acceleration along with the overall fusion and radiation metrics for DT operations are also captured in the full conference presentation tables. The ion ring major radius at final implosion stagnation reaches the millimeters scale and at GeV-level azimuthal energies for protons, deuterons and

tritons. With respect to the fusion/radiation parameters, the peak x-ray and DT fusion neutron yield reach 3.5MJ and 6.6x10^18 neutrons per pulse, respectively, with an overall scientific gain of >19.

D. RHED Physics & Metric Engineering

In addition to the fusion energy and x-ray/neutron radiation applications, the WARP Reactor is also primed for accessing new RHED. The 60MA DPF plasma liner with embedded GeV-level ion ring appears capable of reaching thousands of Tesla and subsequently multi-TPa pressures. Due to the dramatic compression and acceleration of the charged particle rings and plasma liner/target interactions we may even begin to generate significant plasma metamaterial, Warp, Unruh and Dynamic Casimir effects not to mention copious amounts of synchrotron radiation from electron ring modes of operations. Furthermore, once the charged particle rings become relativistic during the final moments of implosion phase the decrease in ring radius saturates as relativistic mass increases. In other words, flux compression shifts from ring velocity to ring mass or enhanced spacetime coupling. Finally, the WARP Reactor may also provide a means for accessing the Quantum Gravity (QG) domain for verification or invalidation of various proposed theories by probing for any spacetime curvature, gravitational potential and/or frame-dragging effects. With respect to our modified EFE and FOM equations (15)-(19) and Mathematica models, we find a significant enhancement of energy-momentum to spacetime curvature coupling due to plasma metamaterial effects via the Sarfatti "S" field factor; the initiation of direct spacetime metric phase change generated by accelerating and imploding RHED charged particle rings beyond Unruh/Casimir thresholds via the Anderson "A" field factor and QG effects via Sutherland's NQG theory. A table of predicted major results is provided in the conference presentation along with the following FOM result: $C_{\alpha\sigma} \sim 8.64\text{x}10^{4}$ m^{-2}; $\Phi_{\alpha\sigma} \sim 3.35\text{x}10^{-3}$ and $\Omega_{\alpha\sigma} \sim 2.3\text{x}10^{10}$ rad/s.

IX. Conclusion

In conclusion, we envision the WARP Reactor as a more compact, modular and economically viable magneto-inertial fusion device for energy production (i.e. G > 19/pulse, $n\tau \sim 5.2\text{x}10^{21}$ keVs/m^3) or advanced propulsion and/or a super-radiant flash x-ray/neutron source for dynamic radiographic applications (i.e. x-ray/neutron yields per pulse > 3.5MJ/6.6x10^{18}, Average Luminance ~ 10^{25} x-ray photons / s mm^2 mrad^2) along with providing access to new relativistic high energy density physics regimes (i.e. multi-MA, GeV-level charged plasma/particle beam-target interactions at multi-TPa, Unruh, Dynamic Casimir & QG effects). The WARP devices would fulfill the immediate need for an intermediate-level machine for z-pinch, beam and pulsed-power flow studies along with the added benefit of recruiting the next-generation of RHED plasma and accelerator scientists, engineers and technicians. WARP would be an ideal platform for prototyping novel pulsed power architectures for continuous rep-rate nuclear fusion and radiographic movie operations thereby enabling us to continue our collaborations across the DOE/DOD complexes along with forging new university and private industry partners through our Cooperative Research Agreement and Strategic Partnership programs.

Finally, with respect to the Gedankenexperiment "A Twisted Compression of the Ehrenfest Paradox" (provided in companion presentation), we propose the following three methods for enhancing energy-momentum to spacetime curvature coupling: 1. Multi-layer RHED plasma and charged particle ring confinement of THz radiation to create plasma/ring metamaterial effects; 2. Azimuthal acceleration beyond Unruh threshold of multi-pass RHED plasma and charged particle rings to generate Leidenfrost-like vortex layers which create spacetime phase transition; 3. Implosion beyond Casimir threshold of RHED plasma and charged particle rings to generate internal negative energy density which also provides additional confinement mechanism to the >5kT magnetic fields in order to prevent plasma/ring metamaterial rapid disassembly.

Acknowledgment

The authors would like to thank Keith LeChien, Stephen Sampayan and Nathan Meezan for reviews, critical discussions and support. This work was performed under the auspices of the U.S. Department of Energy by Lawrence Livermore National Laboratory under Contract DE-AC52-07NA27344.

References

[1] Michael Gordon Anderson, Pulsed Power-Driven Radiation Source System And Method Using A Wave Accelerated Ring Pinch: The WARP Reactor. United States Patent Application #63/499,928, May 3, 2023.

[2] M. G. Anderson, J. K. Walters, E. M. Anaya and D. A. Max, "Wave Accelerated Ring Pinch eXperiment (WARP-X)," ZNetUS Conference, April 21-22 (2022). https://znetus.eng.ucsd.edu/home/znetus-workshop

[3] Erik W Lentz, "Breaking the warp barrier: hyper-fast solitons in Einstein–Maxwell-plasma theory," Classical and Quantum Gravity 38 075015 (2021). https://doi.org/10.1088/1361-6382/abe692

[4] Glenn, Chance, "Positive Energy Density for the Alcubierre Warp Field Equations Using an RF-Driven Dielectric Resonant Cavity," TechRxiv. Preprint. https://doi.org/10.36227/techrxiv.19224552.v1

[5] Jack Sarfatti, "Lectures in Metric Engineering Physics," Academia, August 4, (2022). https://www.academia.edu/83953289

[6] Roderick Sutherland, "Naive Quantum Gravity," General Relativity and Quantum Cosmology (gr-qc); Quantum Physics (quant-ph), (2019). https://doi.org/10.48550/arXiv.1502.02058

[7] Vitaly Bystritskii, Frank J. Wessel, Norman Rostoker, Hafiz Rahman, "Novel Staged Z-Pinch Concept as Super Radiant X-Ray Source for ICF," Current Trends in International Fusion Research pp 347-364, (1997). https://doi.org/10.1007/978-1-4615-5867-5_22

[8] W. A. Stygar, K. R. LeChien, et al., "Impedance-matched Marx generators," Physical Review Accelerator and Beams Volume 20, 040402 – April (2017). https://doi.org/10.1103/PhysRevAccelBeams.20.040402

[9] Leckbee, Joshua, Oliver, Bryan V, Toury, Martial, Cartier, Frederic, and Caron, Michel "Two pulses tests with a single LTD cavity," Sandia National Lab Report SAND2012-9031C United States (2012). https://www.osti.gov/biblio/1062277

[10] B. N. Turman, et al., "PBFA II: A 100 TW Pulsed Power Driver for the Inertial Confinement Fusion Program," Sandia National Lab Report, June (1985) https://apps.dtic.mil/sti/pdfs/ADA638630.pdf

[11] Ryan D. McBride and Stephen A. Slutz, "A semi-analytic model of magnetized liner inertial fusion," Physics of Plasmas 22, 052708 (2015). https://doi.org/10.1063/1.4918953

[12] M. Anderson, et al., "Propagation of intense plasma and ion beams across B-field in vacuum and magnetized plasma," Laser and Particle Beams, vol.23 ,2005, pp.117-129, Cambridge University Press. https://doi.org/10.1017/S0263034605050202

[13] Michael Anderson, Vitaly Bystritskii, Kurt Walters, et al., "Colliding Tori Fusion Reactor," IEEE International Power Modulator and High Voltage Conference in San Diego, CA June 3 - 7 (2012). https://www.nessengr.com/ipmhvc2012